Electronic Supplementary Information

In situ creation of catalytic multiphase and multiscale surroundings for remarkable hydrogen storage performance of MgH_2

Lingchao Zhang,[a] Xin Zhang,[ab] Wenxuan Zhang,[a] Fang Fang*[c], Juan Li[d], Jianjiang Hu[e], Changdong Gu[a], Wenping Sun[a], Mingxia Gao[a], Hongge Pan*[af], Yongfeng Liu*[abf]

[a]State Key Laboratory of Silicon and Advanced Semiconductor Materials and Engineering, Zhejiang University, Hangzhou 310058, China. E-mail address: mselyf@zju.edu.cn

[b]Taizhou Institute of Zhejiang University, Taizhou 318000, China.

[c]Department of Materials Science, Fudan University, Shanghai, 200433 China. E-mail address: f_fang@fudan.edu.cn

[d]College of Materials Science and Engineering, Zhejiang University of Technology, Hangzhou, 310014, China

[e]School of Chemistry and Chemical Engineering, Yantai University, Yantai, 264005, China

[f]Institute of Science and Technology for New Energy, Xi'an Technological University, Xi'an, 710021, China. E-mail address: hgpan@zju.edu.cn

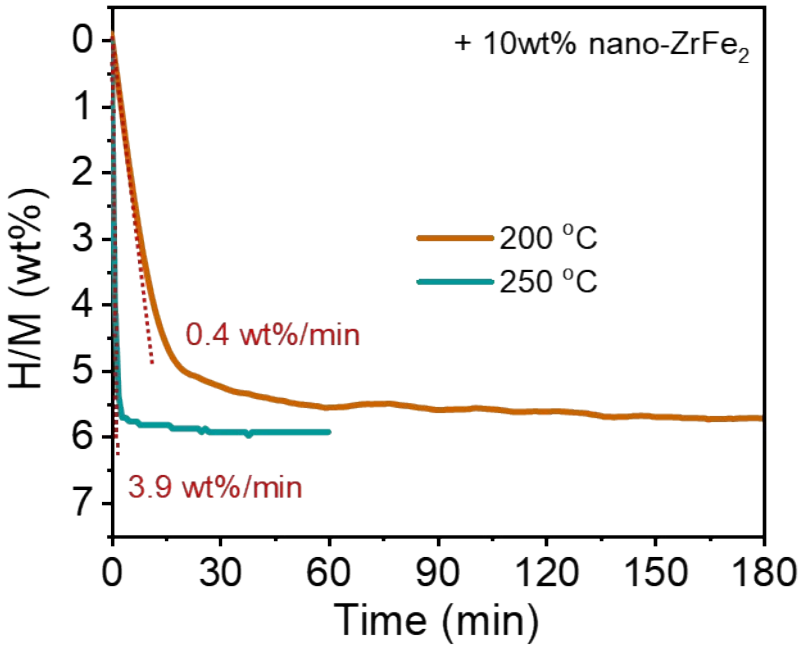

Fig. S1. Isothermal desorption curves of the sample with 10 wt% nano-$ZrFe_2$ at 200 ºC and 250 ºC.

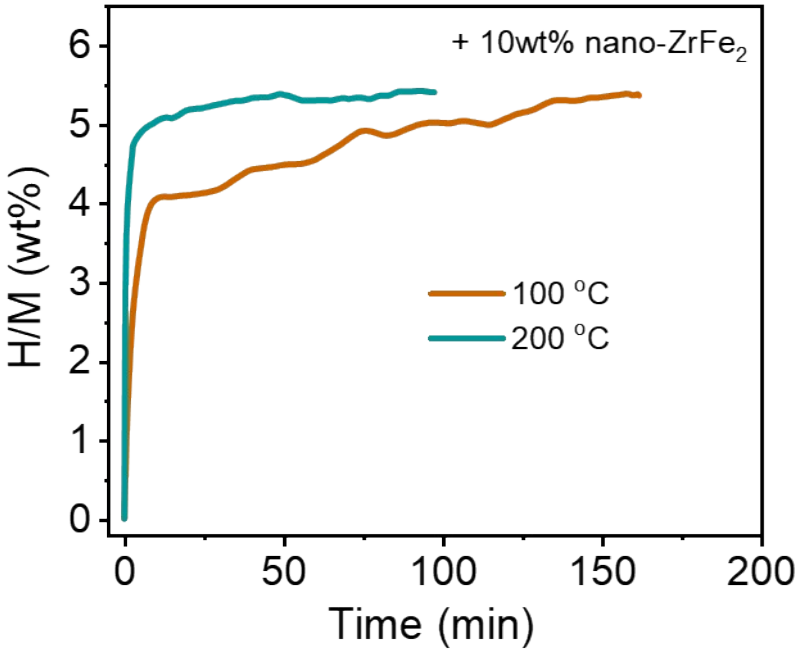

Fig. S2. Isothermal hydrogenation curves of the dehydrogenated sample with 10 wt% nano-$ZrFe_2$ at 100 ºC and 200 ºC.

Table S1. The weight and atomic percentage of Mg, Zr and Fe calculated from EDS results shown in Fig. 4

Element	Line type	10 wt% nano-$ZrFe_2$ (wt%)	10 wt% nano-$ZrFe_2$ (mol%)	10wt% bulk-$ZrFe_2$ (wt%)	10wt% bulk-$ZrFe_2$ (mol%)
Mg	K-line	89.38	95.90	90.97	96.45
Fe	K-line	5.86	2.74	5.58	2.58
Zr	L-line	4.76	1.36	3.45	0.97
Amount		100	100	100	100

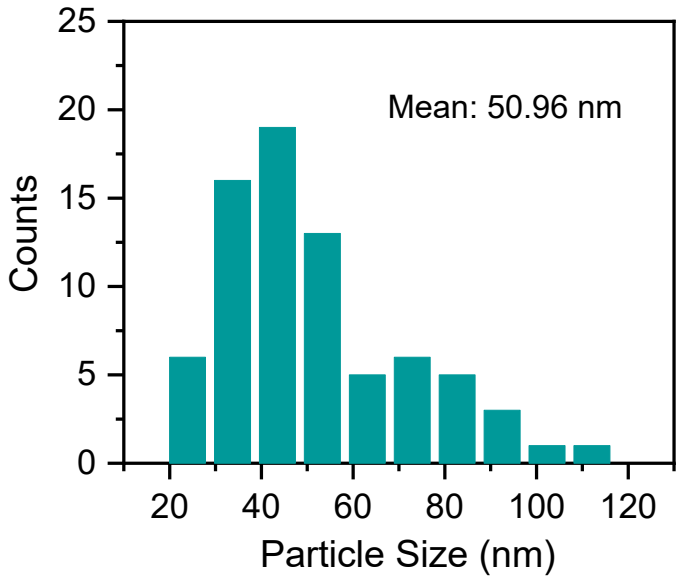

Fig. S3. The particle size distribution of nano-$ZrFe_2$ after ball milling shown in Fig. 4b

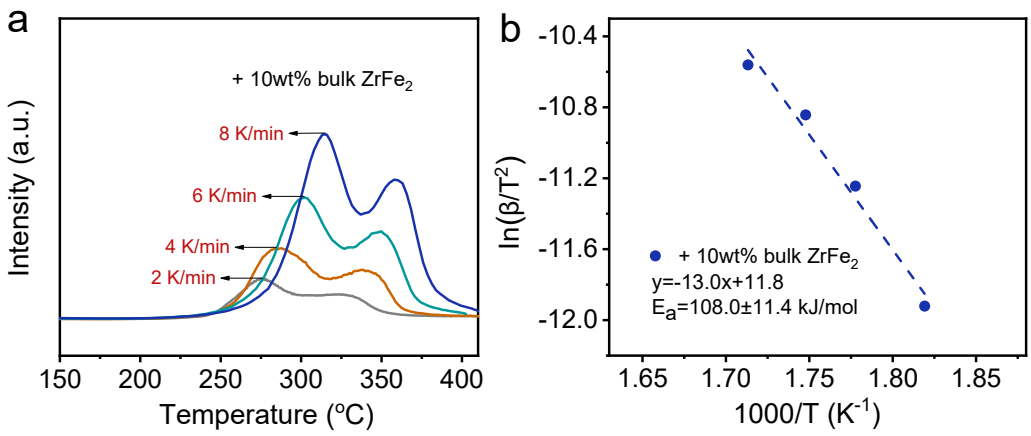

Fig. S4. TPD curves (a) and post-fitted Kissinger's plots (b) of MgH_2 + 10 wt% bulk-$ZrFe_2$ sample under different heating rates.

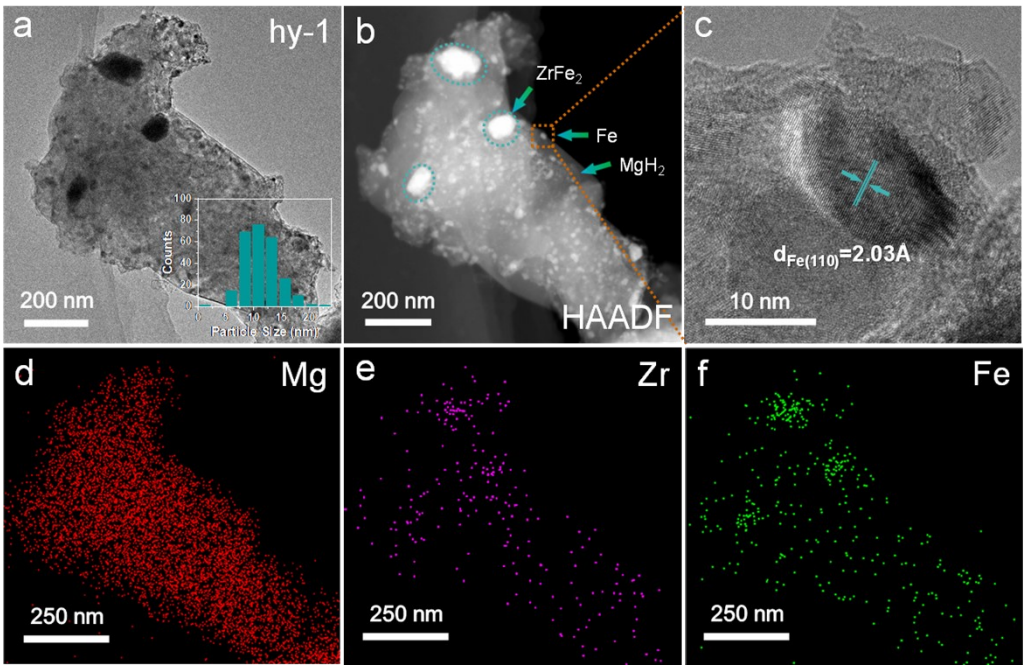

Fig. S5. TEM (a), HAADF (b), HRTEM (c) images and corresponding EDS mappings (d-f) of the hydrogenated MgH_2 + 10 wt% nano-$ZrFe_2$ composite. The inset of (a) is Fe particles size distribution.

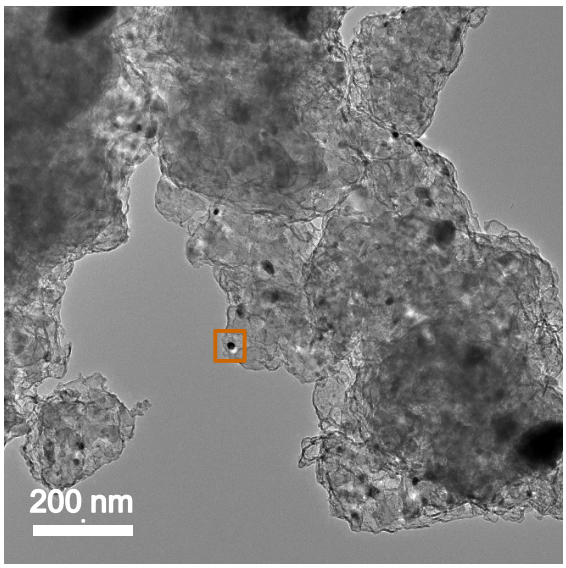

Fig. S6. Low-magnification TEM image of the MgH_2 + 10 wt% nano-$ZrFe_2$ composite dehydrogenated at 250 °C. The marked-out area is the particle shown in Fig. 8.

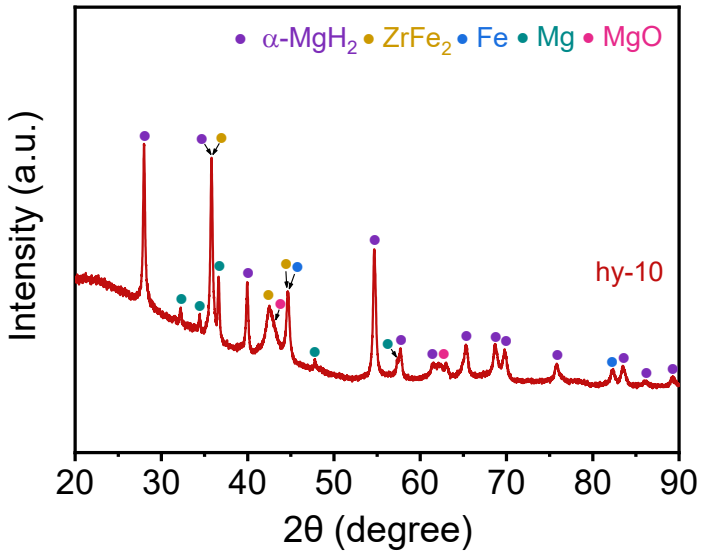

Fig. S7. XRD pattern of the nano-$ZrFe_2$-containing sample after 10 cycles.

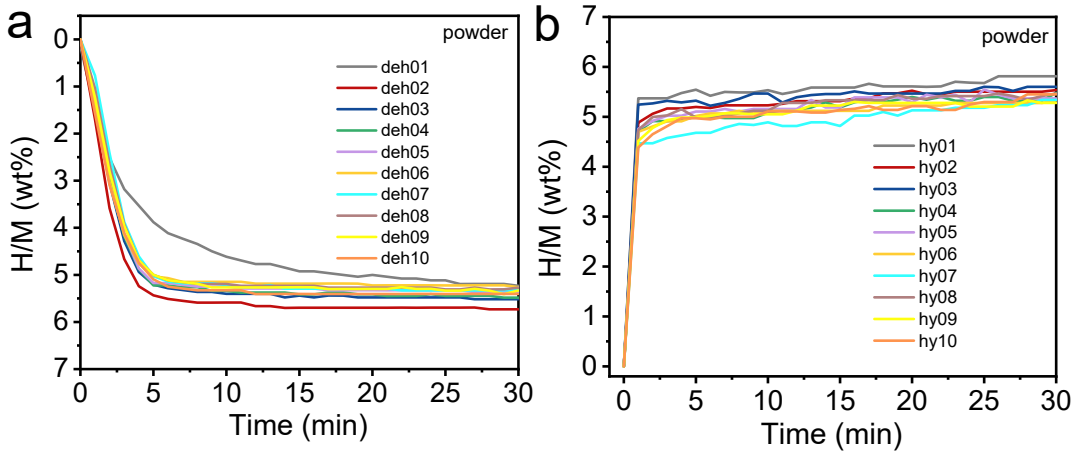

Fig. S8. Comparative analysis of isothermal hydrogen desorption (a) and absorption (b) curves during cycling at 250 °C of the MgH_2 + 10 wt% nano-$ZrFe_2$ powder sample.

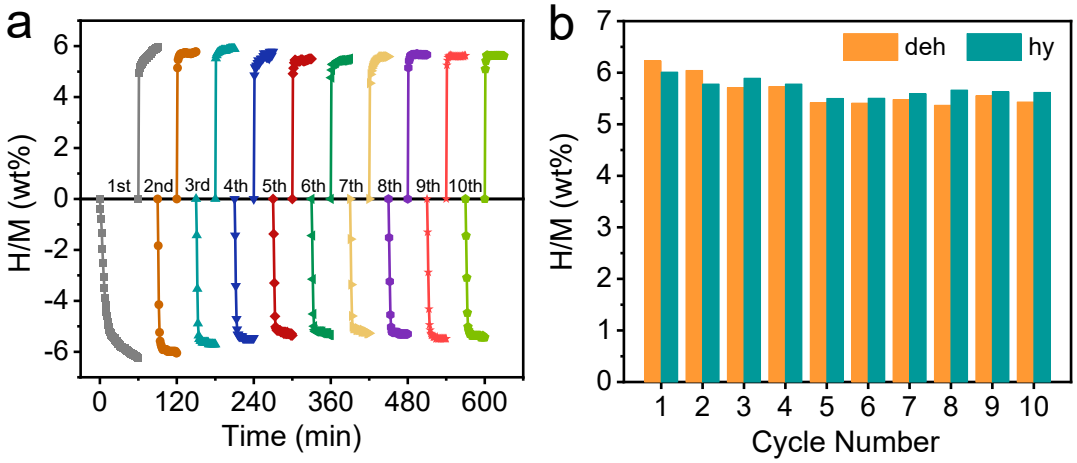

Fig. S9. Isothermal hydrogen absorption and desorption cycling curves at 250 °C (a) and the cycling capacity (b) of the MgH_2 + 10 wt% nano-$ZrFe_2$ pellet sample.

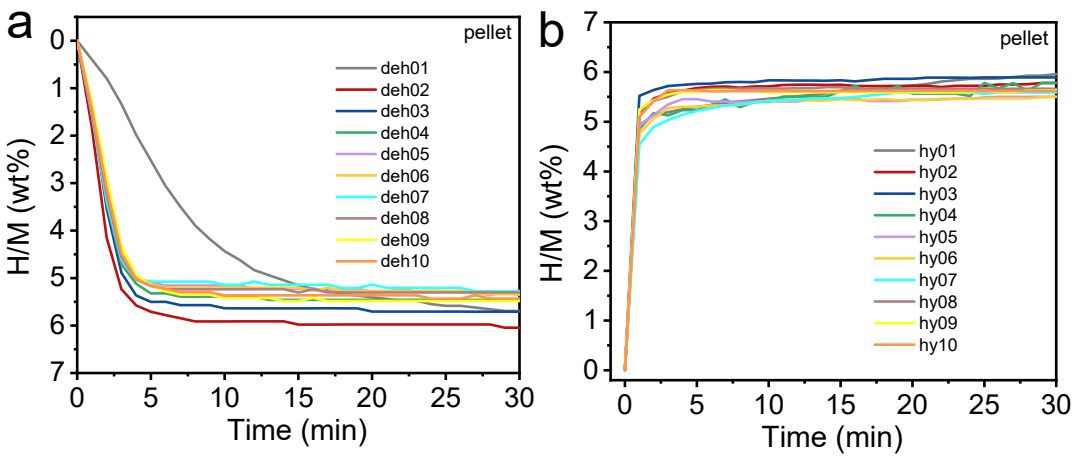

Fig. S10. Comparative analysis of isothermal hydrogen desorption (a) and absorption (b) curves during cycling at 250 °C of the MgH_2 + 10 wt% nano-$ZrFe_2$ pellet sample.

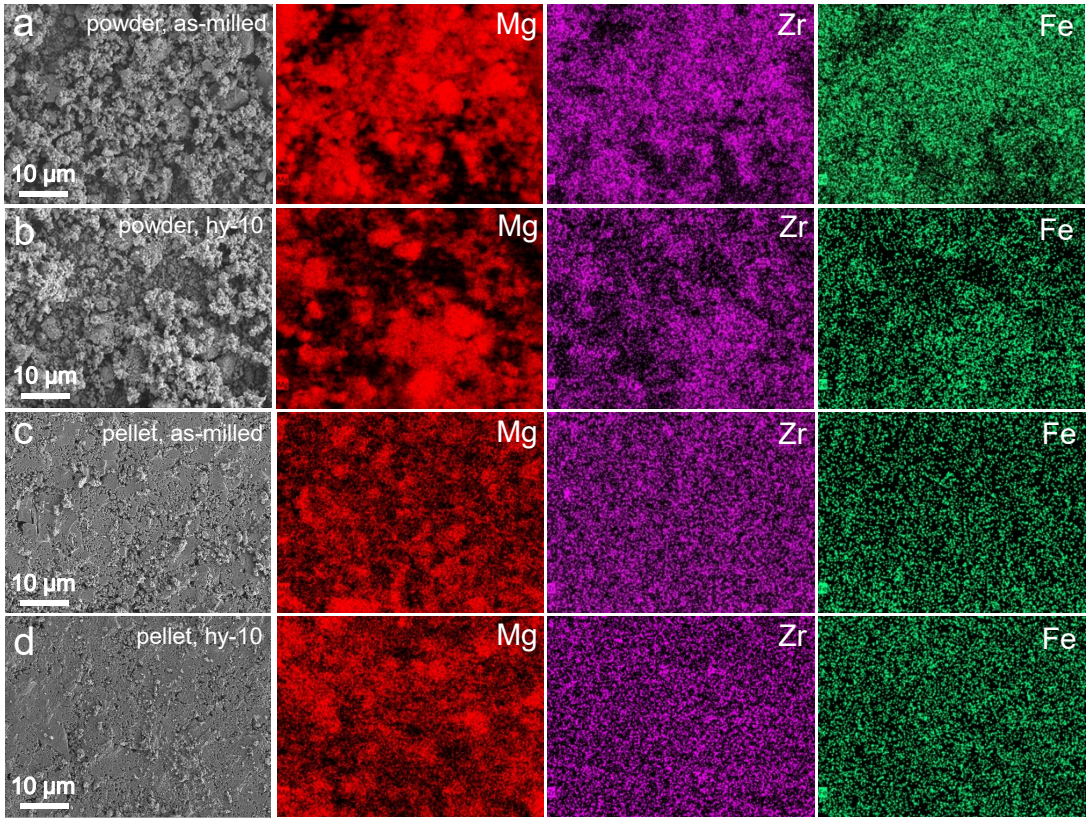

Fig. S11. SEM images and EDS mappings of Mg, Zr and Fe for the as-milled (a, c) and the 10th hydrogenated MgH_2 + 10 wt% nano-$ZrFe_2$ samples (b, d) in powder form (a, b) and cold-pressed pellet (c, d).